Interaction of O_2 with Gold Clusters: Molecular and Dissociative Adsorption

Bokwon Yoon, Hannu Häkkinen,* and Uzi Landman

School of Physics, Georgia Institute of Technology, Atlanta, Georgia 30332-0430

Received: December 2, 2002; In Final Form: February 14, 2003

The interaction of O_2 with charged and neutral gold clusters, Au_N^- and Au_N containing up to eight atoms, investigated through the use of density functional theory with generalized gradient corrections and scalar relativistic pseudopotentials, exhibits a pronounced sensitivity to the cluster size and to its charge state. Molecular adsorption is found to be favorable regardless of the charge state for clusters with $N \leq 3$, while dissociative adsorption is favored for larger clusters. The dissociation process involves a significant barrier (1 eV or more), and it is predicted to result in a large structural distortion in the host gold cluster. The interaction energy is largest for the anionic gold clusters where it exhibits an odd−even alternation as a function of the number of gold atoms, with the maxima occurring for $Au_NO_2^-$ complexes with even N. The molecular bonding mechanism to these complexes involves charge transfer to the oxygen molecule with a concomitant activation of the O−O bond to a superoxo-like state.

1. Introduction

The chemical reactivity of gas-phase metal clusters (mainly transition metals) toward various molecules has been the subject of numerous investigations, motivated by the intrinsic interest in clusters as novel nanoscale catalysts, as well as by the lessons that may be learnt from such studies pertaining to catalysis by supported metal clusters and the adsorption and reactivity mechanisms of extended metal surfaces. Recently there has been a growing interest in the chemical properties of gold nanoclusters and their potential use as nanocatalysts. Some of the key findings in this area may be summarized as follows.

(i) In early experiments[1,2] a definite pattern of oxygen adsorption to negatively charged small gold clusters has been detected, where only anionic clusters with an even number of atoms (odd number of valence electrons) showed significant O_2 uptake, whereas odd-numbered clusters either did not exhibit any propensity for reaction with oxygen[1] or showed very weak reactivity close to the detection limit of the experiment.[2] These early findings have been supported by later studies by two independent groups.[3,4] Neutral clusters and positively charged ones were found to be inert toward oxygen uptake, with the sole exception of Au_{10}^+.[1]

(ii) Gold cluster anions that show a propensity for oxygen adsorption can also coadsorb carbon monoxide,[5−7] thus suggesting them as possible model catalysts for the CO oxidation reaction. Indeed, such a reaction was theoretically predicted for Au_2^- [5] and later confirmed experimentally.[7]

(iii) Recent mobility experiments[8] indicate that pure gold cluster anions prefer *planar* ground-state structures up to surprisingly large sizes (from the experiments the 2D-3D transition size was deduced to be $N = 12$). Very recent high-resolution photoelectron data measured for gold cluster anions can also be interpreted by planar cluster structures up to about $N = 13$.[9] This remarkable propensity for 2D optimal structures has been recently shown[10] to be correlated with the uniquely strong relativistic effects on bonding in gold.[11]

(iv) Supported size-selected gold clusters exhibit remarkable atom-by-atom size-sensitivity in catalyzing the CO oxidation reaction. Furthermore, the active clusters catalyze the reaction well below room temperature. Specifically, it was found for mass-selected deposited gold clusters on a MgO(001) surface, i.e., Au_N/MgO ($2 \leq N \leq 20$), that only clusters with $N \geq 8$ were active in the low-temperature oxidation of CO.[12] Theoretical calculations revealed the following important factors concerning the "nanocatalytic" behavior of supported gold clusters: (1) gold clusters are most likely to be adsorbed on color centers (oxygen vacancies) on the MgO(100) surface; (2) the interaction with the color center involves partial electron transfer (0.5e in the case of Au_8/MgO) to gold; (3) the cluster size, the charge transfer, and the cluster−surface interaction determine the width and the position of the gold d-band in the energy region ($E_F - 7$) eV $< E < E_F$, which in turn induces subtle effects in the details of the binding and activation modes of an oxygen molecule by the gold cluster;[12,13] and (4) structural dynamic fluxionality of the cluster plays an important role in the adsorption of the reactants and in lowering the reaction activation barriers. These findings[13] provide guidelines to understand the chemical activity of larger nanoscale gold particles.[14−16]

Here we report on a systematic theoretical investigation, using density-functional theory, of the adsorption of the oxygen molecule on neutral and charged clusters containing up to to eight gold atoms; while our focus is on anionic clusters, we will also discuss neutral and cationic ones. Overall, we find the adsorption of O_2 to gold clusters to be highly sensitive to the cluster's size and to its charge state. We predict that there is a size-dependent change in the thermodynamically most stable adsorption mode—that is, for both anionic and neutral gold clusters molecular adsorption (MA)[17] is favorable for $N \leq 3$ and dissociative adsorption (DA) is preferred for $N \geq 4$. For anionic clusters, the binding energy to oxygen, $E_B(O_2)$, is predicted to exhibit strong odd−even oscillations, with the value of $E_B(O_2)$ being 0.5−1 eV higher for even-numbered (open electron-shell) clusters than for the neighboring odd-numbered (closed electron-shell) clusters. For neutral clusters, $E_B(O_2)$ is generally 0.5−1 eV smaller than for the corresponding anions. The stronger binding in the MA mode occurs for $Au_NO_2^-$ complexes with even N, and it is accompanied by activation of

10.1021/jp027596s CCC: $25.00
Published on Web 04/18/2003

the O−O bond length to about 1.35 Å, which is a typical value for a superoxo state, involving charge transfer to one of the empty $2\pi^*$ orbitals. The calculated O−O stretch frequency in this state is about 1200 cm^{-1}. In contrast to the MA mode, the dissociative adsorption mode is accompanied by large changes in the structure of the metal host. In all cases the energy-optimal configurations of $Au_NO_2^-$ and Au_NO_2 clusters have planar or near-planar structures up to the largest size studied here ($N = 8$).[18]

2. Theoretical Method

In this study the Kohn−Sham (KS) equations were solved using the Born−Oppenheimer local-spin-density molecular dynamics (BO−LSD−MD) method,[19] including self-consistent generalized gradient corrections (GGA),[20] with nonlocal norm-conserving pseudopotentials[21] for the $5d^{10}6s^1$ and $2s^22p^4$ valence electrons of gold and oxygen atoms, respectively, with scalar-relativistic treatment for gold.[5] The BO−LSD−MD method is particularly suited for this study, since it does not employ periodic replication of the ionic system (that is, no supercell is used) thus allowing accurate calculations on both neutral and charged systems.[19] The KS orbitals are expanded in a plane-wave basis with a 62 Ry energy cutoff, ensuring convergence of the calculated values. No constraints on spin or spatial symmetry were imposed on the structural optimization of the clusters, which used a steepest-descent-like method. The vibrational frequencies of the molecularly adsorbed species were determined from constant energy first-principles MD simulations, starting from the minimum energy configuration but with a stretched (by 1%) interatomic bond length. The calculated bond lengths and binding energies for the elemental dimers Au_2, Au_2^-, AuO, and AuO^- and for the O_2 molecule compare favorably with the experimental data;[5] for example, the calculated dissociation energy of free O_2 is 5.36 eV, in agreement with the measured value of 5.23 eV (see citation 17 in ref 5).

For selected clusters, the barrier for O_2 dissociation was mapped by using the regular "nudged elastic band" (NEB) method.[22] Between the fixed initial (MA) and final (DA) states, a trial reaction path is constructed from a number of intermediate configurations generated by linear interpolation of the coordinates of all the atoms. The NEB method finds the minimum energy path (MEP) between the initial and final states by optimizing the intermediate configurations within two constraints: (i) the adjacent configurations are "kept together" by an elastic spring force, and (ii) each configuration is locally optimized in the direction normal to the path. These optimized intermediate configurations and the corresponding energies define the MEP and the energy barrier. In our case the use of typically six intermediate configurations along the MEP yielded an estimate for the top of the barrier within an accuracy of 0.1 eV.

3. Results

3.1. Anionic $Au_NO_2^-$ Complexes: Molecular vs Dissociative Adsorption. The structural and energetic details of the anionic complexes $Au_NO_2^-$, $2 \le N \le 8$, are displayed in Table 1 and in Figures 1 and 2. For each cluster size, several possible isomers for MA and DA complexes were optimized and a few of the lowest-energy structures are shown in Figure 1. From an inspection of Figure 1, two observations can be made concerning the structures of the MA and DA complexes: (i) the structures are planar or near-planar, with the sole exception of the DA complex for $N = 3$ (structure 3b), and (ii) while the MA mode induces only minor relaxation in the host gold cluster, the DA is always accompanied by major structural changes in the gold part, particularly for $N \ge 5$ (see structures **5a**, **6a**, **7a**, and **8a** in Figure 1). A common structural motif induced by the DA mode is the formation of the (almost) linear chain Au−O−Au with an Au−O bond length of 1.96−1.99 Å and a strong elongation or even a breakage of some nearby Au−Au bonds.

TABLE 1: Calculated Energies for Molecular and Dissociative Adsorption (MA and DA, Respectively) of O_2 to Au_N Clusters[a]

		$Au_NO_2^-$						Au_NO_2		
	A	$E_B(O_2)$ (eV)	d_{O-O} (Å)	ω (cm^{-1})	vDE (eV)	aDE (eV)	spin	$E_B(O_2)$ (eV)	d_{O-O} (Å)	spin
2a	MA	1.39	1.343	1205	3.25	2.93	0.5	0.46	1.285	1
2b	DA	0.79			3.31	3.20	1.5	−0.39		1
3a	MA	0.46	1.304	1347	3.72	3.42	1	0.66	1.277	0.5
3b	DA	0.14			3.36	3.15	0	0.61		0.5
4a	DA	1.79			3.58	3. 45	0.5	1.01		1
4b	MA	1.01	1.328	1217	3.49	3.37	0.5	0.30	1.291	1
4c	MA	0.94	1.335				1.5			
4d	MA	0.93	1.326				0.5			
5a	DA	1.33			3.73	3.39	1	1.00		0.5
5b	MA	0.61	1.316	1292	3.36	3.29	1	0.38	1.285	0.5
5c	MA	0.48	1.493				0			
6a	DA	2.11			3.69	3.55	0.5	0.79		1
6b	MA	1.06	1.362	1216	3.27	3.04	0.5	0.24	1.268	1
6c	MA	1.02	1.355				0.5			
7a	DA	1.30			3.57	3.42	1	1.18		0.5
7b	MA	0.53	1.318	1340	3.72	3.66	1	0.17	1.283	0.5
8a	DA	1.77			4.15	4.09	0.5	0.57		1
8b	DA	1.38					0.5			
8c	MA	0.87	1.330	1290	3.57	3.47	0.5	0.28	1.280	1

[a] Additionally, the inter-oxygen bond lengths (d_{O-O}) for the MA states are given. The geometries of the clusters are labeled in the left column with the notation as defined in Figure 1. The binding energy of O_2 to the cluster is denoted by $E_B(O_2)$, ω is the O−O vibrational frequency (for MA), and vDE (aDE) are the vertical (adiabatic) electron detachment energies from the adsorption complex. In the column marked "spin", we give the spin polarization of the corresponding cluster, that is half of the difference between the number of electrons with up-spin and the number of down-spin electrons. The negative $E_B(O_2)$ value for structure **2b** of Au_2O_2 means that this configuration is not energetically favorable with respect to separated Au_2 and O_2 although it is binding with respect to two oxygen atoms initially in the gas phase. The calculated vibrational frequency of the free O_2 molecule is 1485 cm^{-1} compared to the experimental value of 1580 cm^{-1}. The ω values reported here include a scaling factor of 1580/1485.

The binding energy of the oxygen molecule to the gold cluster anions, $E_B(O_2) = E(Au_N^-) + E(O_2) - E(Au_NO_2^-)$, shows large odd-$N$/even-$N$ oscillations as a function of the cluster size (see Figure 2). For the MA mode the maximum binding energy occurs for the gold dimer anion (1.39 eV) while for $N = 4$, 6, and 8 $E_B(O_2)$ is of the order of 0.8−1 eV, with weaker binding found for the clusters with $N = 3$, 5, and 7 for which $E_B(O_2)$ is about 0.5 eV. For $N \ge 4$, dissociative adsorption is energetically favorable over the molecular adsorption, and in the DA mode, the maximum value of $E_B(O_2)$ (2.1 eV) occurs for $N = 6$.

The vertical (vDE) and adiabatic (aDE) electron detachment energies for $Au_NO_2^-$ complexes are plotted in Figure 3, parts a and b for the DA and MA modes, respectively. The vDE and aDE values vary typically in the range 3−4 eV and miss the distinct odd−even oscillations found by us earlier for the pure gold cluster anions.[9,23] Local maxima in the vDE are observed for $N = 5$ and $N = 8$ for the DA complexes, and for $N = 3$ and $N = 7$ for the MA complexes. The relaxation energy (vDE − aDE) varies between 0.1 and 0.3 eV, with the largest values occurring for $N = 3$ and 5 for the DA complexes and $N = 2$, 3, and 6 for the MA ones.

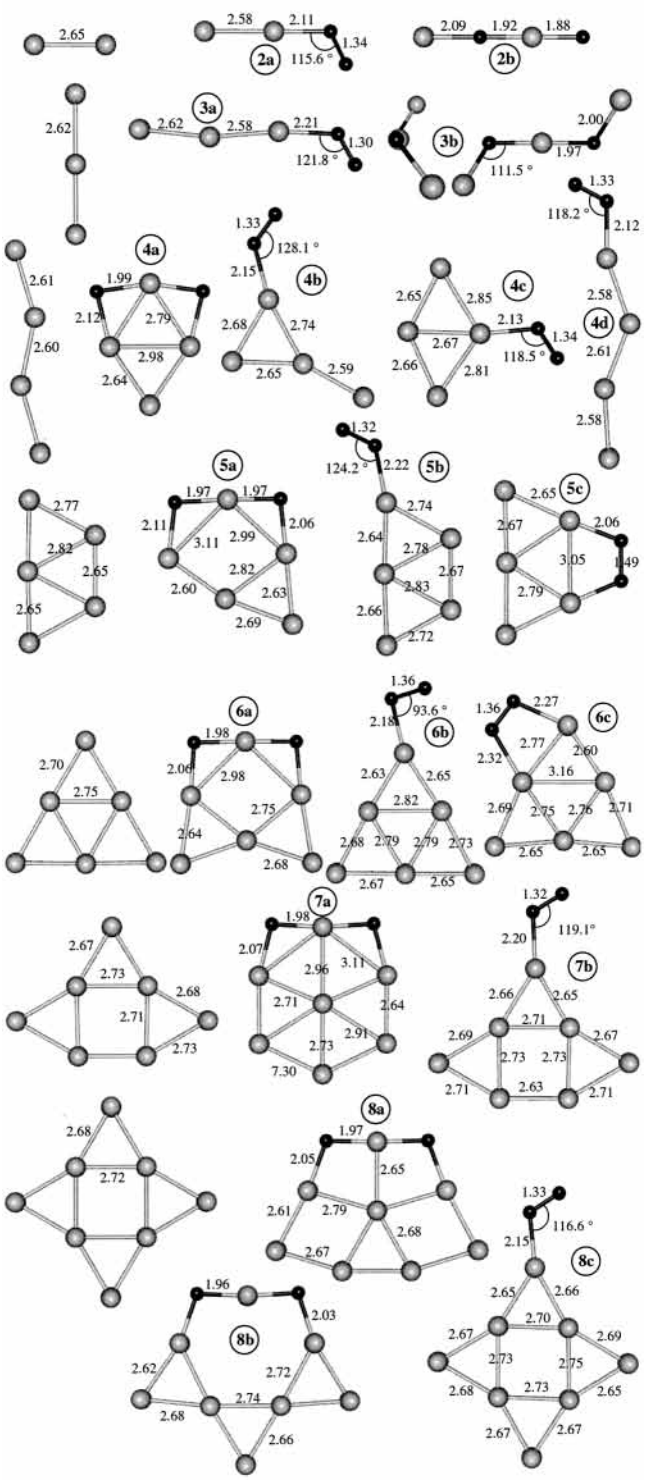

Figure 1. Optimized structures of $Au_NO_2^-$, $2 \leq N \leq 8$. The ground-state structures of the corresponding pure gold cluster anions are given on the left. The bond lengths are given in angstroms.

Finally, in the column marked "spin" in Table 1 we give the spin polarization of the corresponding cluster, that is half of the difference between the number of electrons with up-spin and the number of down-spin electrons. Note that for the anionic MA complexes with an odd number of gold atoms a minimum of 0.5 appears, whereas for an even number of gold atoms a spin of 1 is found (i.e., two unpaired electrons), correlating with the nonactivated state of the adsorbed O_2 molecule for these clusters (see below).

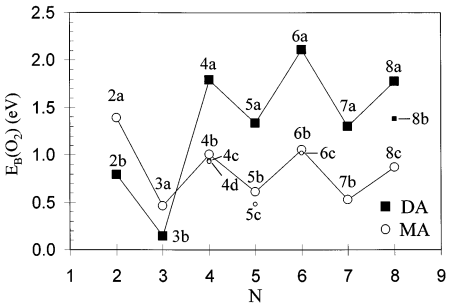

Figure 2. Binding energy of an oxygen molecule to gold cluster anions. *N* is the number of gold atoms in the cluster. The structures are labeled as in Figure 1. The dissociative adsorption (DA) mode and the molecular adsorption (MA) one, are denoted by a filled square and an empty circle, respectively.

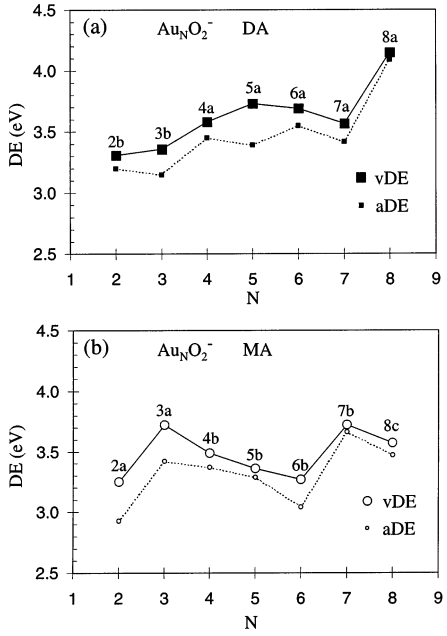

Figure 3. Vertical and adiabatic electron detachment energies (vDE and aDE, respectively) for the dissociatively (a) and molecularly (b) adsorbed $Au_NO_2^-$ complexes (DA and MA, respectively). The labeling of the structures is as in Figure 1. In part a, large and small filled squares correspond, respectively, to vDE and aDE values, and in part b, the vDE and aDE values are depicted by the open large and small circles, respectively.

3.2. Neutral Au_NO_2 Complexes. The binding energies of O_2 in neutral Au_NO_2 complexes are given in Table 1 and Figure 4; here, we note that since our major focus in this study is on anionic clusters we did not search extensively for the lowest energy configurations of the neutral adsorption complexes, limiting ourselves to structural optimizations starting from the ground state configurations found for the corresponding negatively charged ones. For both the MA and DA complexes the binding energies are generally smaller than for the corresponding anionic complex. However, for the DA complexes with $N = 4-7$, the binding energy is still at least 0.8 eV. For the neutral MA complexes, the maximum binding energy occurs for $N = 3$ (0.6 eV), and it gradually decreases for larger clusters. For $N \geq 4$, the DA mode is preferred over the MA one. As before we show also in Table 1 the spin polarization of the Au_NO_2 complexes.

3.3. Correlation between the Activation of O_2 and the Charge State of the Complex. As shown in Table 1, the longest O−O bonds occur in MA complexes, $Au_NO_2^-$, with even *N*

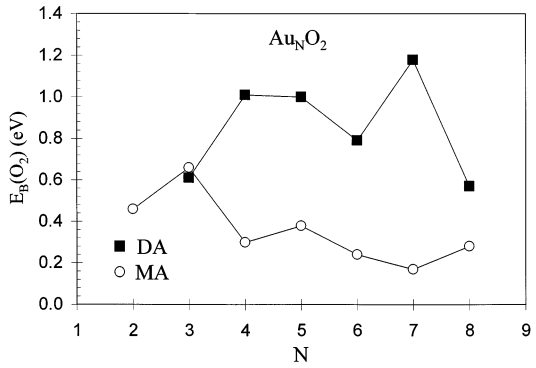

Figure 4. Binding energies of an oxygen molecule to neutral gold clusters, Au_NO_2. Filled squares and empty circles correspond to calculated DA and MA values, respectively.

(odd number of electrons), the typical values being about 1.35 Å. To further analyze the bonding and activation mechanism we display in Figure 5a the local density of electronic states (LDOS) of the MA $Au_6O_2^-$ complex (see structure 6b in Figure 1), projected onto the O_2 molecule and the gold part of the complex. All the prominent peaks of the LDOS spectrum corresponding to the adsorbed O_2 molecule can be assigned to KS orbitals displaying characters of the free molecular oxygen (see the orbitals depicted in Figure 5a). Bonding of the molecule to gold involves hybridization of the 5σ, $1\pi_\perp$, and $1\pi_{||}$ states with the lower-energy edge (5−7 eV below the Fermi energy) of the gold d-band; here and in the following we use the terminology common in the solid-state literature (e.g., Fermi energy and d-band), even though the states of the clusters are discrete as they are in molecules. Close to E_F, the up-spin $2\pi_\perp$* and $2\pi_{||}$* and the down-spin $2\pi_{||}$* states are occupied. Analysis of the local charge shows an excess charge of 0.75e on the oxygen, and this charge is mainly promoted to the down-spin $2\pi_{||}$* state, rendering the adsorbed oxygen molecule as a superoxo-like species with a stretched O−O bond length of 1.362 Å. In Figure 5b, we display an iso-surface plot of the local spin polarization (i.e., the local difference between the spin-up and spin-down electron densities). Note that the spin polarization plot for the oxygen part is similar to the electron distribution of the up-spin $2\pi_\perp$*. This is due to the cancellation of the polarization between the up and down spin $2\pi_{||}$* orbitals in the superoxo-like state, and the fact that the down-spin $2\pi_\perp$* orbital is unoccupied; i.e, it is the lowest unoccupied molecular orbital (LUMO), depicted by the right-most peak in the bottom panel of the LDOS shown in Figure 5a.

In the LDOS of the corresponding neutral Au_6O_2 complex (Figure 6a), the down-spin $2\pi_{||}$* and $2\pi_\perp$* orbitals are both empty (i.e., they are located above the Fermi energy) the molecule possesses the free-molecule spin $S = 1$, and the bond length is 1.268 Å, i.e., merely 0.018 Å longer than the calculated value of free O_2 (1.25 Å). This indicates lack of activation of the O_2 molecule by the neutral gold cluster. The above picture of bonding is supported by the spin-polarization iso-surface shown in Figure 6b. Indeed, the cylindrically symmetric shape (about O−O bond) of the spin-polarization plot, which is similar to the spin-polarization iso-surface corresponding to the free oxygen molecule, originates from addition of the densities of the occupied up-spin $2\pi_{||}$* and $2\pi_\perp$* orbitals and the aforementioned unoccupancy of the corresponding down-spin−orbitals.

We note also that since the spin-down antibonding $2\pi_{||}$* orbital which is occupied in the case of $Au_6O_2^-$ is of *bonding* nature between the oxygen and gold atoms, the anionic complex is able to bind O_2 stronger than the neutral one, where this orbital

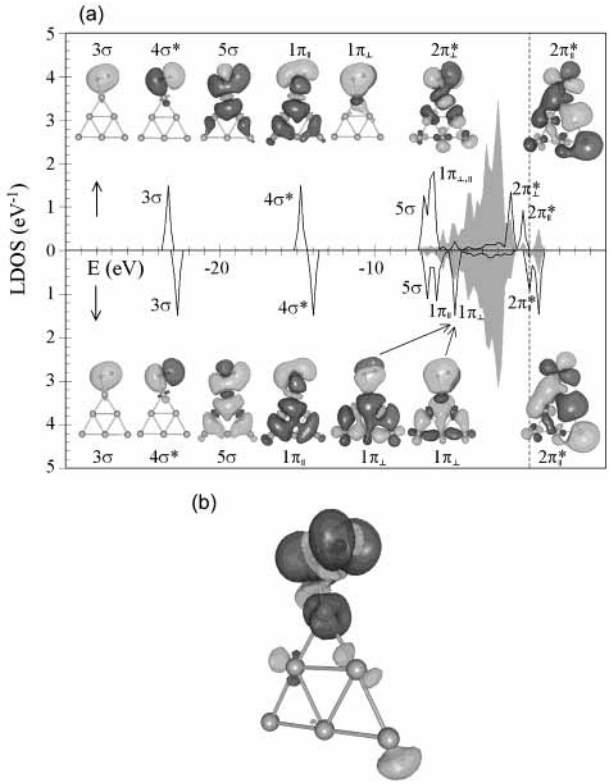

Figure 5. (a) Local density of electronic states (LDOS) projected on the O_2 molecule (solid line) in the MA $Au_6O_2^-$ complex (see structure **6b** in Figure 1). The KS orbitals corresponding to the prominent peaks display clear characteristics of the free O_2 molecular orbitals in the oxygen part. The LDOS of the gold part is shown by the gray shaded curve. The highest occupied orbital (HOMO) is at zero. For the 1π and 2π state manifolds, the "parallel" (||) notation refers to the orbitals where the π-character close to the oxygen molecule lies in the plane defined by the gold cluster. The location of the Fermi level is indicated on the horizontal axis by a dashed vertical line at 0 eV. Note that here both the up-spin $2\pi_{||}$* and $2\pi_\perp$* orbitals, as well as the down-spin $2\pi_{||}$* orbital, are occupied (i.e., located below the Fermi energy), while the down-spin $2\pi_\perp$* is the LUMO state depicted by the rightmost peak in the bottom panel of the LDOS. (b) Isosurface of the local spin polarization (i.e., the local difference between the spin-up and spin-down electron densities). Note that the spin polarization plot is similar to the electron distribution of the up-spin $2\pi_\perp$* in the oxygen part . This is due to the cancellation of the polarization between the up- and down- spin $2\pi_{||}$* orbitals in the superoxo-like state, and the fact that the down-spin $2\pi_\perp$* orbital is unoccupied.

is empty (compare the corresponding binding energies of 1.06 and 0.24 eV in Table 1). This kind of bonding and activation mechanism was discussed by us previously in the context of a gold cluster adsorbed on a color center on a MgO surface, where the color center donates electron charge to the adsorbed gold cluster making it partially (0.5e in the case of Au_8/MgO) negatively charged and facilitating binding and activation of molecular oxygen to a peroxo state.[12,13] Activated peroxo-like and superoxo-like states of O_2 were also observed as precursor states in the disssociative adsorption of oxygen on the Pt(111) surface.[24]

The magnitude of the charge transfer and the concomitant bond activation is expected to be largest for those $Au_NO_2^-$ complexes where the electron detachment from the gold part requires the least amount of energy. This is indeed the case, as shown in Figure 7 which displays and correlates the calculated vertical electron detachment energy[9,23] of the gold cluster anions Au_N, $2 \le N \le 8$, with the calculated excess charge in the oxygen part of the MA $Au_NO_2^-$, the O−O bond length, and the O−O

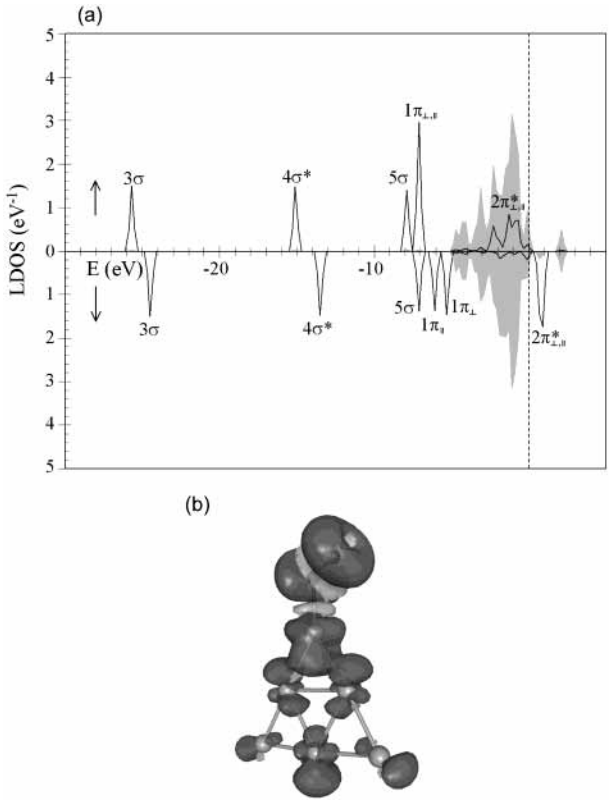

Figure 6. (a) Same as Figure 5, but for Au_NO_2. Note that here both the down-spin $2\pi_\perp$* and $2\pi_{||}$* orbitals are unoccupied (i.e, they are located above the Fermi energy). (b) Isosurface of the local spin polarization (i.e., the local difference between the spin-up and spin-down electron densities). Note the cylindrically symmetric shape (about the O−O bond) of the spin-polarization plot in the oxygen part, originating from the addition of the densities of the occupied the occupied up-spin $2\pi_{||}$* and $2\pi_\perp$* orbitals, and the aforementioned unoccupancy of the corresponding down-spin−orbitals.

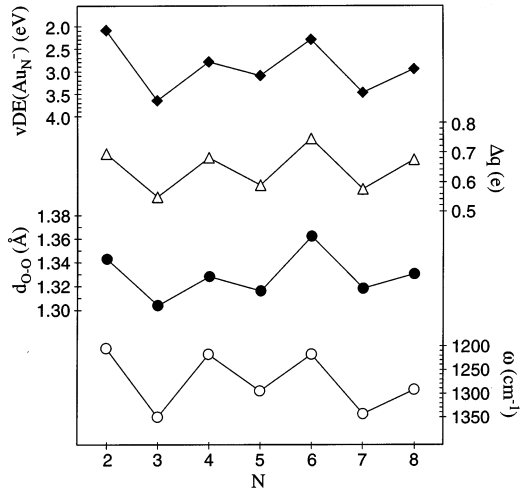

Figure 7. Correlations between the vertical electron detachment energy (vDE) of the bare gold cluster anion Au_N^-, the amount of charge transferred to the oxygen molecule (Δq, in units of the electron charge e) in the MA $Au_NO_2^-$ complex, the O−O bond length (d_{O-O}), and the O−O bond stretch frequency (ω).

bond stretch frequency ω. Low electron detachment energy leads to a larger charge transfer to oxygen, which in turn stretches and weakens (activates) the O−O bond and lowers the O−O bond stretch frequency. The predicted values of ω for the MA complexes are between 1200 and 1350 cm^{-1} with minimum values (around 1200 cm^{-1}) for clusters with $N = 2$, 4, and 6

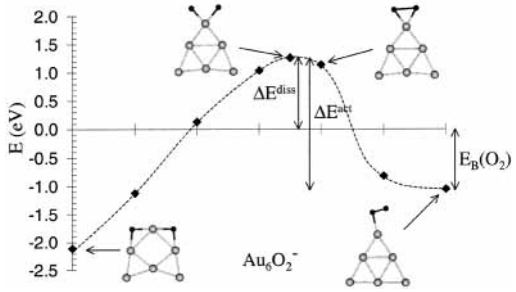

Figure 8. Activation and dissociation barriers for O_2 interacting with Au_6^-. The dashed line is plotted for visual guidance. For numerical values see Table 2. The filled diamond denotes calculated values for the locally optimized configurations along the minimum energy path. The horizontal axis denotes the "reaction coordinate".

TABLE 2: Amount of Charge Transferred to the Adsorbed Oxygen Molecule (Δq (e)), the Binding of O_2 to the Gold Cluster, the Dissociation Barrier (ΔE^{diss}), and the Activation Barrier (ΔE^{act})[a]

	Δq (e)	$E_B(O_2)$ (eV)	ΔE^{diss} (eV)	ΔE^{act} (eV)
$Au_5O_2^-$	0.588	0.61	1.42	2.03
$Au_6O_2^-$	0.745	1.06	1.27	2.33
Au_6O_2	0.321	0.24	3.10	3.34
$Au_6O_2^+$	0.143	0.46	3.15	3.61

[a] Results are shown for $Au_5O_2^-$ and for the anionic, neutral, and cationic Au_6O_2 cluster. For definitions of the barriers, see Figure 8.

gold atoms. These predictions could be tested by high-resolution photoelectron spectroscopy.

We also analyzed the bonding and activation of the oxygen molecule in the cationic MA $Au_6O_2^+$ complex in light of the above discussion. The calculated values for the binding energy of O_2 (0.46 eV), the O−O bond length (1.26 Å), the O−O stretch frequency 1514 cm^{-1}, and the vertical ionization potential of the complex (7.98 eV), indicate that although the positively charged gold cluster can bind O_2 (even slightly stronger than the neutral cluster), it fails to activate the O−O bond. Analysis of the corresponding LDOS (not shown) confirms the lack of activation (absence of charge promotion to the spin-down 2π* manifold). Furthermore, the close correspondence between the vIP of the Au_6O_2 complex (7.98 eV) and the vIP of the neutral bare Au_6 cluster (8.13 eV) indicates that ionization of the neutral Au_6O_2 complex involves electron removal mainly from the gold part of the complex.

3.4. Barrier for Dissociation of the O_2 Molecule. The barriers for O_2 dissociation were mapped by using the regular "nudged elastic band" method[22] for $Au_5O_2^-$, $Au_6O_2^-$, Au_6O_2, and $Au_6O_2^+$. As the dissociated state of oxygen yields the ground state of each of these adsorption complexes, the general shape of the barrier in all cases is similar to that shown in Figure 8 for $Au_6O_2^-$. The pertinent energies (the binding energy of the initial molecular state, the maximum value of the barrier over the dissociation limit, and the activation energy) are denoted in Figure 8 and are displayed in Table 2. The smallest dissociation barrier, the top of which is located around an O−O distance of about 2.5 Å, occurs for $Au_6O_2^-$ (1.27 eV), which together with the molecular binding energy of 1.06 eV yields an activation energy of 2.33 eV. We note that for the neutral Au_6O_2 and cationic $Au_6O_2^+$ complexes both the barrier height and the activation energy are very high, well over 3 eV.

In light of the calculated high energy (2.33 eV) required for activation of the molecularly adsorbed species we have investigated other competing reaction channels. Our results are summarized in Table 3. Apart from the simple back-reaction

TABLE 3: Calculated Activation Energy for Possible Reaction Channels of Processes Starting from the $Au_6O_2^-$MA Complex[a]

reaction channel	ΔE^{act} (eV)
$Au_6O_2^-(MA) \rightarrow Au_6^- + O_2$	1.06
$Au_6O_2^-(MA) \rightarrow Au_6O_2^-(DA)$	2.33
$Au_6O_2^-(MA) \rightarrow Au_5O_2^-(MA) + Au$	2.60
$Au_6O_2^-(MA) \rightarrow Au_5O_2(MA) + Au^-$	3.46
$Au_6O_2^-(MA) \rightarrow Au_4O_2^-(MA) + Au_2$	2.57
$Au_6O_2^-(MA) \rightarrow Au_4O_2(MA) + Au_2^-$	3.92

[a] Note that all the reactions shown in the table are endothermic. MA and DA correspond to the molecularly adsorbed and dissociatively adsorbed species.

(desorption of O_2 back to the gas phase), all the considered channels involving fragmentation of the gold part of the complex require even higher energies than the calculated activation energy for O_2 dissociation.

4. Summary

We have presented an extensive and systematic study on the interaction of the oxygen molecule with gas-phase gold clusters in the size range of two to eight gold atoms. Our findings are summarized as follows.

(1) The interaction energy is largest for the anionic gold clusters where it presents a distinct odd−even behavior as a function of the number of gold atoms, the maxima occurring for even-N $Au_NO_2^-$ complexes.

(2) The bonding mechanism involves charge transfer to the oxygen molecule with a concomitant activation of the O−O bond to a superoxo state. The activation is strongest for even-N $Au_NO_2^-$ complexes where the O−O bond stretching frequency is close to 1200 cm^{-1}.

(3) We predict a change in the energetically optimal adsorption mode as a function of the size of the gold cluster: clusters with less or equal than three atoms prefer molecular adsorption whereas dissociative adsorption of oxygen is preferred for the larger clusters.

(4) The dissociation barriers are quite large, of the order of 1 eV or more over the desorption limit $E(Au_N^-) + E(O_2)$, and observation of dissociative oxygen adsorpion may require special experimental conditions, such as photodissociation of O_2 in conjunction with forming the gold clusters, or the interaction of anionic gold clusters with a beam of atomic oxygen or ozone.

(5) The dissociative adsorption is predicted to induce large relaxations in the gold part of the complex which could be detected by mobility measurements or electron diffraction spectroscopy. Furthermore, high-resolution photoelectron spectroscopy should in this case reveal typical Au−O bond frequencies (our calculated values are in the range 500−600 cm^{-1}).

(6) Neutral and cationic gold clusters also bind oxygen, although the interaction is much weaker and does not induce O−O bond activation.

The information provided by this study, pertaining to the energetics and mechanisms of the interaction processes of O_2 with small gold clusters and the size-dependent patterns which we have described, could provide the impetus for further experimental studies on the interaction of oxygen with gold clusters and it's direct implications to the nanocatalytic activity of these clusters in the gas phase and when supported on oxide surfaces.

Acknowledgment. This research is supported by the U.S. Air Force Office of Scientific Research. The calculations were performed at the GIT Center for Computational Materials Science.

Note Added in Proof. After the acceptance of our manuscript, experimental vibrational-resolved photoelectron spectra from $Au_NO_2^-$ with $N = 2$ and $N = 4$ appeared (see Stolcic, D. et al., *J. Am. Chem. Soc.* **2003**, *125*, 2848). From Figure 2 in that paper, the vibrational splitting of the lowest-binding-energy peak corresponds to O−O frequencies of 1444 cm^{-1} (179 meV) for $N = 2$, and 1226 cm^{-1} (152 meV) for $N = 4$. While the former frequency agrees well with our predicted value of 1426 cm^{-1} for the neutral MA Au_2O_2 complex (i.e., the final state of the electron detachment process), the latter corresponds to that of the initial anionic MA complex $Au_4O_2^-$ where our predicted value is 1217 cm^{-1} (see Table 1). The absence of features corresponding to the final-state (neutral) in the photoelectron spectra for $Au_4O_2^-$ may be correlated to the weaker predicted binding of O_2 in the neutral Au_4O_2 complex compared to that in Au_2O_2 (the O_2 binding energies to the neutral tetramer and dimer gold clusters are 0.30 eV and 0.46 eV, respectively, see Table 1). Associated with the weaker binding of O_2 to the cluster is a higher probability for O_2 desorption from the neutral Au_4O_2 complex following electron photodetachment from $Au_4O_2^-$.

References and Notes

(1) Cox, D. M.; Brickman, R.; Creegan, K.; Kaldor, A *Z. Phys. D* **1991**, *19*, 353; Cox, D. M.; Brickman, R.; Creegan, K. A. *Mater. Res. Soc. Symp. Proc.* **1991**, *206*, 34.

(2) Lee, T. H.; Ervin, K. M. *J. Phys. Chem.* **1994**, *98*, 10023.

(3) Salisbury, B. E.; Wallace, W. T.; Whetten, R. L. *Chem. Phys.* **2000**, *262*, 131.

(4) Hagen, J.; Socaciu, L. D.; Elijazyfer, M.; Heiz, U.; Bernhardt, T. M.; Wöste, L. *Phys. Chem. Chem. Phys.* **2002**, *4*, 1707.

(5) Häkkinen, H.; Landman, U. *J. Am. Chem. Soc.* **2001**, *123*, 9704.

(6) Wallace, W. T.; Whetten, R. L. *J. Am. Chem. Soc.* **2002**, *124*, 7499.

(7) Socaciu, L. D.; Hagen, J.; Bernhardt, T. M.; Wöste, L.; Heiz, U.; Häkkinen, H.; Landman, U. Submitted to *J. Am. Chem. Soc.*

(8) Furche, F.; Ahlrichs, R.; Weis, P.; Jacob, C.; Gilb, S.; Bierweiler, T.; Kappes, M. *J. Chem. Phys.* **2002**, *117*, 6982.

(9) Häkkinen, H.; Yoon, B.; Landman, U.; Li, X.; Zhai, H.-J.; Wang, L. S. To be published.

(10) Häkkinen, H.; Moseler, M.; Landman, U. *Phys. Rev. Lett.* **2002**, *89*, 033401.

(11) Pyykkö, P. *Chem. Rev.* **1988**, *88*, 563.

(12) Sanchez, A.; Abbet, S.; Heiz, U.; Schneider, W.-D.; Häkkinen, H.; Barnett, R. N.; Landman, U. *J. Phys. Chem. A* **1999**, *103*, 9573.

(13) Häkkinen, H.; Abbet, S.; Sanchez, A.; Heiz, U.; Landman, U. *Angew. Chem. Int. Ed.* **2003**, *42*, 1297.

(14) Haruta, M. *Catal. Today* **1997**, *36*, 153.

(15) Bond, G. C.; Thompson, D. T. *Catal. Rev.—Sci. Eng.* **1999**, *41*, 319.

(16) Valden, M.; Lai, X.; Goodman, D. W. *Science* **1998**, *281*, 1647.

(17) For a recent theoretical study of neutral and anionic Au_NO_2 clusters with $N = 2-5$ and limited to molecular adsorption, see: Mills, G.; Gordon, M. S.; Metiu, H. *Chem. Phys. Lett.* **2002**, *359*, 493.

(18) Here we note that for $Au_NO_2^-$ with $N = 5-8$ several three-dimensional structures have been tested by us, and they were found to be higher-energy isomers compared to the 2D structures.

(19) Barnett, R. N.; Landman, U. *Phys. Rev. B* **1993**, *48*, 2081.

(20) Perdew, J. P.; Burke, K.; Ernzerhof, M. *Phys. Rev. Lett.* **1996**, *77*, 3865.

(21) Troullier, N.; J. L. Martins, J. L. *Phys. Rev. B* **1991**, *43*, 1993.

(22) Mills, G.; Jónsson, H.; Schenter, G. K. *Surf. Sci.* **1995**, *324*, 305.

(23) Häkkinen, H.; Landman, U. *Phys. Rev. B.* **2000**, *62*, R2287.

(24) Eichler, A.; Hafner, J. *Phys. Rev. Lett.* **1997**, *79*, 4481.